JOURNAL OF SOLID STATE CHEMISTRY 107, 524–538 (1993)

Structure and Physical Properties of the $LnBa_2Cu_2MO_{7+\delta}$ System (Ln = Rare Earth and Y; M = Ga, Co)*

T. A. MARY, N. R. S. KUMAR, AND U. V. VARADARAJU

Materials Science Research Centre, Indian Institute of Technology, Madras 600 036, India

Received September 3, 1992; in revised form January 28, 1993; accepted March 2, 1993

A series of compounds with the general formula $LnBa_2Cu_2GaO_{7+\delta}$ (Ln = La–Gd, Y) and $LnBa_2Cu_2CoO_{7+\delta}$ (Ln = La–Yb, Y) have been synthesized and characterized. The phase formation is found to be sensitive to the size of the rare earth ion in both the series. For Ln = La–Eu, the Ga-substituted compounds are single phase and possess tetragonal Y-123 structure. In the $LnBa_2Cu_2CoO_{7+\delta}$ series, single-phase formation is noted for all the Ln's studied except Yb. An orthorhombic-to-tetragonal transition occurs across the rare earth series. For Ln = La–Er and Y, the phases are orthorhombic, and for Ln = Tm the phase is tetragonal. Oxygen content of the phases is found to be ~7.0 for the $LnBa_2Cu_2GaO_{7+\delta}$ series, whereas for the $LnBa_2Cu_2CoO_{7+\delta}$ system, the value increases to ~7.25 as expected. Electrical resistivity studies show that all the phases are semiconducting with activation energies in the range 0.03–0.28 eV. IR spectra and magnetic susceptibility of select compounds have been studied and discussed.

Introduction

The high-temperature superconductor, $YBa_2Cu_3O_7$ (Y-123, T_c = 90 K) crystallizes in an orthorhombically distorted oxygen-deficient tripled perovskite structure with a = 3.82, b = 3.88, and c = 11.67 Å. In Y-123, yttrium has an 8-fold and barium has a 10-fold coordination of oxygens. There are no oxygens in the Y-plane. The two Ba sites are equivalent. In the structure two distinct, crystallographically inequivalent sites exist for the copper: The Cu(1) site has a square planar coordination of oxygens with 2 × Cu(1)–O(1) = 1.94 Å and 2 × Cu(1)–O(4) = 1.85 Å. The Cu(2) site has a square pyramidal coordination with 2 × Cu(2)–O(2) = 1.93 Å, 2 × Cu(2)–O(3) = 1.96 Å, and 1 × Cu(2)–O(4) = 2.30 Å. There are five distinct sites for oxygen: O(1) along the b-axis in the basal plane; O(2) and O(3) parallel to the a- and b-axes, respectively, in the CuO_2 square planes; O(4) bridging the CuO_2 plane and CuO chain; and O(5) positioned along the a-axis in the basal plane (*1–4*).

In the orthorhombic Y-123 with O_7 stoichiometry, the oxygens are ordered in the basal plane with all the O(1) positions filled and O(5) positions vacant. The oxygen in the basal plane can be selectively removed (deintercalated) leading to compositions varying from O_7 to O_6. The degree of orthorhombicity decreases as we go from compositions with O_7 to O_6 due to disordering of the oxygen occupancy between O(1) and O(5) positions. The structure eventually transforms to tetragonal symmetry at ~$O_{6.35}$. Careful structural studies on Y-123 with varying oxygen stoichiometries have revealed the existence of superstructures for specific values of the oxygen stoichiometry, e.g., the phase with $O_{6.5}$ is an oxygen-vacancy-ordered orthorhombic II structure with O(1) sites being occupied in alternating chains (along the b-axis) ($a' = 2a$); similarly, the $O_{6.75}$ phase also appears to have a

* Forms part of the Ph.D. thesis submitted by TAM to IIT, Madras.

0022-4596/93 $5.00

vacancy-ordered structure (*5–7*). The orthorhombic → tetragonal transformation can also be achieved by increasing the oxygen content above 7.0. The excess oxygen occupies the O(5) position in addition to the fully occupied O(1) positions of the O_7 composition. The $O_{7+\delta}$ can be achieved by suitable chemical substitution at the Ba/Cu sites (*8, 9*).

The structure of $YBa_2Cu_3O_7$ is amenable to extensive chemical substitution. Yttrium can be replaced by all rare earths (*Ln*) other than Ce, Tb, and Lu, retaining the orthorhombic tripled perovskite structure. Superconductivity with $T_c \sim 90$ K is exhibited by all *Ln*-123 except when *Ln* = Pr (Pr-123 is semiconducting). The Ba-site can be substituted by Sr to the extent of $x = 1.25$ in $YBa_{2-x}Sr_xCu_3O_7$. The unit cell parameters decrease with increasing x and T_c is suppressed marginally (0.4 K/at%) (*1–4*).

Substitution at the Cu-site by transition and nontransition elements has been extensively studied. It is generally agreed that trivalent ions (e.g., Fe^{+3}, Co^{+3}) substitute preferentially at the Cu(1)-site for lower concentrations of the substituent, and for higher concentrations, substitution takes place at the Cu(2)-site also (*10–12*). On the other hand, divalent ions (e.g., Ni^{+2}, Zn^{+2}) are known to substitute preferentially at the Cu(2)-site (plane site) (*9, 10, 13*). Substitution at the Cu(1)-site by trivalent ions which prefer octahedral coordination leads to consequent uptake and/or disorder of oxygen in the basal plane, and the structure changes to tetragonal symmetry. Divalent ion substitution at the CuO_2 planes does not affect the symmetry, and the orthorhombicity is retained throughout the range of solid solubility. However, in the case of most of the substituents at the Cu-site the solubility is far less than $x = 1.0$ (maximum $x = 0.3$–0.4) in $YBa_2Cu_{3-x}M_xO_7$ except for Co ($x = 1.0$) and Fe ($x = 0.8$) (*10*).

Replacing Ba completely by Sr in Y-123, however, can increase the solubility to $x = 1.0$. Sunshine *et al.* (*14*) have synthesized $YSr_2Cu_2MO_{7+\delta}$ with M = Al, Fe, and Co with a tetragonal structure. Recently, Roth *et al.* (*15*) and Vaughey *et al.* (*16*) reported the synthesis of $LnSr_2Cu_2Ga_1O_7$. There are very few reports of substitution at the Cu-site by ions with valence higher than +3. Murayama *et al.* (*17*) and Greaves and Slater (*18*) have reported the synthesis of $LaBa_2Cu_2TaO_8$, and Rey *et al.* (*19*) synthesized single-phase $LaBa_2Cu_2NbO_8$. In both Nb- and Ta-substituted La-123, TaO_6 and NbO_6 octahedra replace the CuO_4 square planes at the Cu(1)-site. Yaron *et al.* (*20*) have reported the synthesis of $YBa_2Cu_2WO_{9-\delta}$, but the structure is a cation-ordered variant of the cubic perovskite structure and is not considered as a derivative of Y-123.

Recently we have studied the effect of Ga substitution at the Cu-site in the Nd-123 system and found that Ga substitution could be effected up to $x = 1.0$ in $NdBa_2Cu_{3-x}Ga_xO_7$ (*21*). In the Y-123 system, on the other hand, Ga substitution at the Cu-site to a significant level ($x > 0.1$ in $YBa_2Cu_{3-x}Ga_xO_{7+\delta}$) has not been unequivocally established. This prompted us to think that the solid solubility of Ga in the 123 structure depends on the nature and size of the rare earth ion. In the present study we report on the results of the effect of varying the rare earth ion (*Ln*) in the $LnBa_2Cu_2GaO_{7+\delta}$ and $LnBa_2Cu_2CoO_{7+\delta}$ systems on the phase formation, structural and IR spectral features, and electrical and magnetic properties.

Experimental

Phases with the following compositions were synthesized and studied: $LnBa_2Cu_2MO_{7+\delta}$, *Ln* = La–Yb and Y; M = Ga and Co. The compounds were prepared by high-temperature solid-state reaction from high purity oxides: Ln_2O_3 (99.99%; IRE, India; La_2O_3 and Nd_2O_3 (preheated at 950°C/24 hr, cooled, and stored in a desiccator), $BaCO_3$ (99.999%), CuO (99.9%), and Ga_2O_3 (99.999%) (all Cerac), and Co_3O_4 (Fisher Co.). Stoichiometric amounts of the oxides were mixed well and heated at 920°C for 24 hr with intermittent grindings and heated

again at 940°C for 24 hr. The reacted powder was pressed into pellets (8 mm dia, 1–2 mm thick; WC-lined stainless steel die and plunger; hydraulic press; 2–3 tons pressure) and sintered at 940°C for 24 hr in air. In the case of multiphase samples an additional heat treatment at 1000°C for 24 hr has been given. The samples were oxygen treated in a tubular furnace at 900°C for 24 hr, cooled to 600°C, held for 48 hr, and furnace cooled to room temperature in 1 atm oxygen flow. The $LnBa_2Cu_3O_6$ (Ln = Y, Nd) phases were prepared by heating $LnBa_2Cu_3O_7$ powder under vacuum in a quartz tube at 550°C for 2 hr followed by quenching the quartz tube in ice.

The compounds were characterized by powder X-ray diffraction (XRD) (Seifert unit, Germany; CuK_α radiation) and the lattice parameters were obtained by LSQ fitting of the high angle reflections. Oxygen content of the phases was estimated by the iodometric titration method (*21, 22*). The oxygen content values are accurate to ±0.03. For the $LnBa_2Cu_2CoO_{7+\delta}$ phases, far-IR diffuse reflectance spectra were recorded with a Fourier transform IR spectrometer (Bio-Rad, FTS-40V) at room temperature with a resolution of ±0.5 cm^{-1}. The samples in powder form were mixed with polyethylene powder and the spectra were recorded in the range 450–100 cm^{-1}. For $LnBa_2Cu_2GaO_{7+\delta}$ phases, electrical resistivity measurements as a function of temperature (in the range 303–480 K) were done on the pellets by the two-probe method. To ensure good electrical contact the top and bottom portions of the pellets were coated with silver paint (Eltecks Co., Bangalore, India) and dried at 100–110°C in an oven before mounting between the electrodes. The resistivity studies on $LnBa_2Cu_2CoO_{7+\delta}$ phases were done by the four-probe van der Pauw method on the pellets as a function of temperature in the range 300–150 K using a closed-cycle He-refrigerator (CTI-Cryogenics, USA; Model M22). The electrical contacts were given by impregnating indium metal and soldering fine gauge copper wires to the sintered pellets. Magnetic susceptibility measurements were done on select samples of $LnBa_2Cu_2GaO_{7+\delta}$ phases using a SQUID magnetometer (Quantum Design, Model 1822, MPMS) in the range 300–5 K, in a field of 100 G.

Results and Discussion

a. $LnBa_2Cu_2GaO_{7+\delta}$ (Ln = La–Dy, Y) System: Structure and Stoichiometry

Phases with Ln = La, Pr, Nd, Sm, Eu, Gd, and Dy have been synthesized and studied. The phases are black in color. XRD patterns reveal single-phase formation for phases with Ln = Pr, Nd, Sm, and Eu and can be indexed on the basis of a tetragonal cell with 123 structure. Small unidentified lines (10–15% intensity) are observed in the XRD patterns of $GdBa_2Cu_2GaO_{7+\delta}$ along with the major 123-phase lines. For phases with Ln = La, Dy, and Y, the XRD patterns reveal multiphase formation with additional peaks corresponding to Ga_2O_3 and CuO. An additional heat treatment at 1000°C for 24 hr in air followed by oxygen treatment at 900°C/24 hr and 600°C/48 hr and furnace cooling to RT in flowing oxygen has been given to the multiphase samples. $LaBa_2Cu_2GaO_{7+\delta}$ formed a single-phase compound after this additional heat treatment and the XRD patterns did not show any unindexable lines. On the other hand, XRD patterns of phases with Ln = Gd, Dy, and Y remain unchanged even after the additional heat treatment at high temperature (1000°C, 24 hr). This can be explained considering the phase formation behaviour of the simple $LnGaO_3$ perovskites. Whereas the larger Ln^{3+} (Ln = La–Sm) form the $LnGaO_3$ under 1 atm pressure, high pressures are required to stabilize $LnGaO_3$ with smaller Ln's (*21*). The arguments can, therefore, be extended to the present system since the structure is perovskite-related. Thus, the tolerance factor criteria that hold good for simple perovskites can be qualitatively extended to the case of the 123 structure. There is a narrow range of the ionic radius of Ln^{3+} that

TABLE I

STRUCTURAL, ELECTRICAL, AND MAGNETIC DATA FOR $LnBa_2Cu_2GaO_{7+\delta}$ (Ln = La, Pr, Nd, Sm, Eu, and Gd)

Ln	Tetragonal lattice parameters a (Å)	c (Å)	V (Å^3)	$\rho_{300\ K}$ ($\times 10^3$ Ω cm)	E_a (eV) (303–480 K)	δ (±0.03)	μ_B (calc.) (BM)	μ_B (theor.) (BM)
La	3.959	11.96	187.5	0.3	—	—	—	—
Pr	3.927	11.79	181.8	2.6	0.18	0.04	3.26	3.58
Nd	3.921	11.76	180.8	2.5	0.28	0.00	3.20	3.62
Sm	3.909	11.73	179.9	2.2	0.10	0.02	—	—
Eu	3.898	11.69	177.6	2.8	0.21	0.03	—	—
Gd[a]	3.891	11.68	176.8	—	—	0.02	7.31	7.94

[a] Slightly multiphasic; ρ–T data could not be obtained because the pellet crumbled under pressure of the spring-loaded contacts.

stabilizes the 123 structure when one Cu per formula unit is replaced completely by Ga^{3+}.

The XRD patterns of all the single-phase $LnBa_2Cu_2GaO_{7+\delta}$ compounds are similar to that of tetragonal Y-123 (space group: $P4/mmm$). The tetragonal structure is evident from the merger of characteristic orthorhombic (hkl) reflections (e.g., 013, 103; 020, 200, etc.). The lattice parameters a and c obtained by LSQ fitting of high-angle reflections and the unit cell volume show a systematic decrease from Ln = La–Gd as can be expected from the ionic radius considerations (lanthanide contraction) (Table I).

Recently Roth *et al.* (*15*) and Vaughey *et al.* (*16*) reported studies on $LnSr_2Cu_2GaO_7$ (Ln = La–Yb, Y). The space group $Ima2$ which is closely related to $P4/mmm$ as well as $Pmmm$ has been chosen to index the patterns with approximate orthorhombic lattice parameters $a \sim 22.8$, $b \sim 5.5$, and $c \sim 5.4$ Å. The occurrence of ($h10$; h = odd) reflections necessitated the choice of the above unit cell. In the present study, however, no such extra reflections have been noticed in the XRD patterns and all the observed reflections could be indexed on a tetragonal ($P4/mmm$) unit cell. In $LnSr_2Cu_2Ga_1O_7$, the CuO_4 square planar chains (Cu(1)-site) running along the b-axis are replaced by GaO_4 tetrahedral chains running along the diagonal of the basal plane (ab-plane). The oxygen stoichiometry in the above compounds is fixed at 7.0. Our earlier studies on the $NdBa_2Cu_{3-x}Ga_xO_{7+\delta}$ system also showed that the phases are tetragonal for x = 0.1–1.0, and the oxygen content remains unchanged at values close to 7.0 for all values of Ga concentration ($0.0 \leq x \leq 1.0$) (*21*).

In the present study, the oxygen content of all the single phase $LnBa_2Cu_2GaO_{7+\delta}$, estimated by iodometric titration method (*21, 22*), are close to 7.0 (in the range 6.98–7.04) (Table I). This shows that there is no uptake of extra oxygen with Ga substitution. Hence, the disorder of oxygen among O(1) and O(5) positions could be the main reason for the observed tetragonal structure.

b. $LnBa_2Cu_2CoO_{7+\delta}$ (Ln = La–Yb, Y): Structure and Stoichiometry

Phases with Ln = La, Pr, Nd, Sm, Eu, Gd, Dy, Ho, Er, Tm, and Y have been synthesized and studied. The XRD patterns of $LnBa_2Cu_2CoO_{7+\delta}$ compounds reveal single-phase formation except for Ln = Yb. The XRD peaks are sharp indicating well-crystalline nature of the phases. Extra peaks

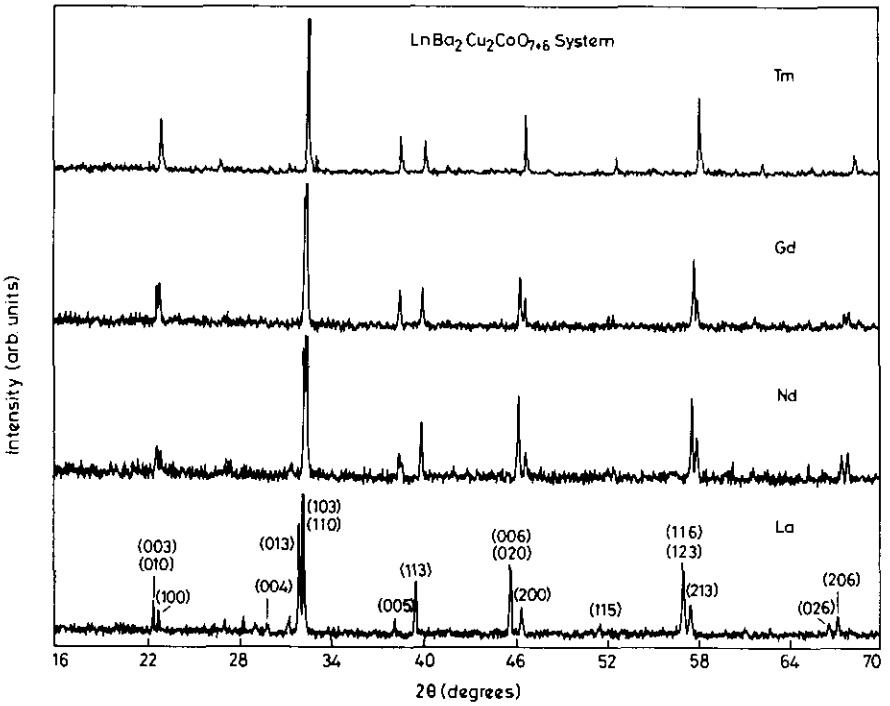

FIG. 1. XRD patterns (CuK_α) of LnBa$_2$Cu$_2$CoO$_{7+\delta}$, Ln = La, Nd, Gd, and Tm, indicating O → T transition across the lanthanide ion.

corresponding to Yb_2BaCuO_5 are observed in addition to those of the major 123-phase in $YbBa_2Cu_2CoO_{7+\delta}$. All the single-phase $LnBa_2Cu_2CoO_{7+\delta}$ are black in color and are stable toward exposure to normal atmospheric conditions. They possess the orthorhombic 123 structure except when Ln = Tm (Fig. 1 and Table II). This is in contrast to the $LnBa_2Cu_2GaO_{7+\delta}$ system which adopts the tetragonal structure. The degree of orthorhombicity [(*b*-*a*)/*a*] is highest for $LaBa_2Cu_2CoO_{7+\delta}$ and $NdBa_2Cu_2CoO_{7+\delta}$ and decreases monotonically with decreasing ionic radius of the Ln^{3+} ion. The orthorhombic lattice parameters *a*, *b*, and *c* obtained by least-squares fitting of high-angle reflections show a systematic decrease from Ln = La–Er as the ionic radius decreases from La^{3+} to Er^{3+}. The unit cell volume also decreases in the above order as expected. $YBa_2Cu_2CoO_{7+\delta}$ is almost tetragonal, whereas $TmBa_2Cu_2CoO_{7+\delta}$ is truly tetragonal (Table II). $YBa_2Cu_2CoO_{7+\delta}$ has been reported earlier (*10*) to be tetragonal with lattice parameters a = 3.89 and c = 11.63 Å.

The oxygen content of the phases estimated by iodometric titration method (*21*, *22*) reveal that the values are in the range 7.20–7.28 for all single-phase $LnBa_2Cu_2CoO_{7+\delta}$, showing an uptake of oxygen with Co substitution in all the cases for charge neutrality. This is in agreement with the results reported earlier for the Y-123 system. The substituted trivalent ions (Fe^{+3}, Co^{+3}) occupy the Cu(1)-site for small concentrations and for higher values of x, the ions occupy the Cu(2)-site also. Square planar coordination is not known for Fe^{3+} and Co^{3+} ion in oxides whereas tetrahedral, square pyramidal, and octahedral coordinations are well known. Bridges *et al.* (*23*) based on XAFS studies on the $YBa_2Cu_{3-x}M_xO_{7+\delta}$ (M = Fe, Co) system proposed that Fe and Co in the basal plane form zig-zag

TABLE II

STRUCTURAL AND ELECTRICAL DATA FOR $LnBa_2Cu_2CoO_{7+\delta}$ (Ln = RARE EARTHS AND Y)

	Ortho./tetra. lattice parameters								
Ln	a (Å)	b (Å)	c (Å)	V (Å)	$(b-a)/a$ (10^{-2})	δ (± 0.03)	$\rho_{300\ K}$ (Ω cm)	$\rho_{150\ K}$ (Ω cm)	$E_{a(150-300\ K)}$ (eV)
La	3.902	3.961	11.87	183.4	1.51	0.28	0.02	0.1	0.03
Pr	3.900	3.938	11.81	181.3	0.97	0.26	17.5	6870	0.16
Nd	3.886	3.927	11.80	180.1	1.06	0.25	4.1	727	0.13
Sm	3.896	3.916	11.76	179.3	0.51	0.20	40.3	13872	0.15
Eu	3.876	3.911	11.74	178.0	0.90	0.28	0.8	123	0.13
Gd	3.882	3.909	11.71	177.8	0.67	0.24	4.8	4732	0.18
Dy	3.871	3.896	11.68	176.2	0.65	0.20	3.1	261	0.13
Ho	3.877	3.889	11.66	175.8	0.31	0.28	0.7	60	0.12
Er	3.870	3.884	11.67	175.4	0.36	0.25	0.7	45	0.11
Tm	3.878	3.878	11.64	175.1	0.00	0.23	2.8	101	0.09
Y	3.888	3.889	11.67	176.1	0.03	0.28	0.1	1	0.06

chains, and the aggregation of these chains will promote twinning which results in the average tetragonal symmetry. In this model the Fe and Co can have oxygen coordination between four and six. Indeed, HREM and electron diffraction measurements (*24–26*) on phases with low Co content ($x \ll 1.0$) revealed the formation of Co containing clusters with Co free microdomains of orthorhombic structure. The random orientation of the microdomains produce an average tetragonal structure in the diffraction experiments.

The additional oxygen has two possible sites to occupy: (i) the O(5) site in the basal plane (along the a-axis) and (ii) in the Y-plane (between the CuO_2 planes; O(6) position). There are no reports of oxygen occupancy in the Y-plane in the Y-123 structure either in the pure or substituted phases. Even in Co- and Fe-substituted Y-123, it is known that for higher concentrations of the substituent the Cu(2)-site is also substituted, but there is no evidence for the presence of oxygen in the Y-plane. Recently, however, Slater *et al.* (*27*) have studied the $LaBa_2Cu_{3-x}Fe_xO_{7+\delta}$ system by neutron diffraction, and they suggest that with increasing Fe content (x), the occupancy of oxygen in the La-plane [O(6)-position] increases with the associated occurrence of O(2) vacancies. The structure, however, remains tetragonal even for $x = 1.0$. The occupancy of O(6) position is correlated with cation disorder between La and Ba. They also find that in the case of Y-123 such a cation disorder is not seen due to the greater size difference between Y^{3+} and Ba^{2+} (compared to that of La^{3+} and Ba^{2+}) ions and no occupancy of the O(6)-sites. There are also reports of oxygen occupancy between the CuO_2 planes in related structures whenever there is a Sr^{2+} ion, but not Ca^{2+} or Y^{3+} ion, e.g., $Bi_2Sr_3Co_2O_{8+\delta}$ (*3, 28*) and $La_2SrCu_2O_6$ (*29*).

Recently, in our studies on $NdBa_2Cu_{3-x}M_xO_{7+\delta}$ (M = Fe, Co, Ni, Zn) system (*30*) we found that the structure transforms to tetragonal symmetry as M concentration increases: for $x \geq 0.08$ the phases are tetragonal when M = Fe and Co, and for $x \geq 0.5$ the phases are tetragonal when M = Ni and Zn. However, for M = Fe and Co, with increasing x, the structure once again transforms to orthorhombic symmetry for $x \geq 0.5$. The systematic changes in the lattice parameters, the O → T → O transition with increasing x and the absence of any impurity peaks in the XRD patterns rule out the possibility of incomplete substitution of Co at the

Cu-site. This observation has been corroborated recently by Hegde *et al.* (*31*) during their studies on the $PrBa_2Cu_2CoO_{7+\delta}$ system. They speculate that the Co occupies the Cu(2)-site exclusively and the excess oxygen is accommodated at the O(6) position. This will leave the CuO chains intact and hence the observed orthorhombicity. However, the observation of the O → T transition indicates that part of the Co indeed occupies the Cu(1)-site for phases with $x \leq 0.4$ above which the T → O transition is observed. However, there is no special driving force (heating in reducing atmosphere etc.) for the migration of all the Co from the Cu(1)-site to the Cu(2)-site for phases with $x > 0.5$. Thus, the assumption that all the Co occupies the Cu(2)-site is not fully justified.

Alternatively, for higher concentration of Co, as in the present study, enhanced clustering of Co, leaving large undoped domains of 123 with CuO chains intact and thereby giving rise to orthorhombicity may be possible. However, this picture still can not explain the decreasing degree of orthorhombicity with decreasing size of the Ln^{3+} ion and the tetragonality of $TmBa_2Cu_2CoO_{7+\delta}$. It is also possible that a superstructure exists and the weak superstructure reflections could not be seen in our XRD patterns. Further studies (electron or neutron diffraction, HREM, etc.) are required to understand the detailed nature of the crystal structure of these phases.

c. Far-Infrared Studies on $LnBa_2Cu_2CoO_{7+\delta}$

Far-infrared spectra (IR) of superconducting orthorhombic $YBa_2Cu_3O_7$ and semiconducting tetragonal $YBa_2Cu_3O_6$ have been reported in the literature (*32–38*). Group theory predicts 21 infrared active modes for orthorhombic $YBa_2Cu_3O_7$, out of which only 5 are clearly identified. This is probably due to the high electrical conductivity within the CuO_2 planes which screens the phonons confined to these planes. The mean values of the well defined IR bands, along with the uncertainties are at 152 ± 3, 191 ± 8, 277 ± 7, 312 ± 6, and 565 ± 14 cm^{-1} (*32*). For the tetragonal $YBa_2Cu_3O_6$, 11 infrared active modes were predicted and at least 10 of them have been observed. Removing oxygen from the metallic and superconducting $YBa_2Cu_3O_7$ eventually creates semiconducting material and thereby reduces the screening within the CuO_2-plane and more lattice vibrational modes become visible. The main IR bands observed for $YBa_2Cu_3O_6$ are at 107 ± 2, 118 ± 4, 151 ± 6, 191 ± 3, 215 ± 4, 252 ± 5, 356 ± 4, 440 ± 10, 597 ± 9, and 642 ± 12 cm^{-1} (*32*). Out of the eleven predicted modes, six are doubly degenerate (E_u) and they split into B_{2u} and B_{3u} modes in the orthorhombic phase. Some of these split bands are not seen in the spectra of $YBa_2Cu_3O_7$ due to the anisotropic screening by the conduction electrons as mentioned earlier (*32–38*).

It is reported (*32, 34*) that when Y is replaced by heavier rare earths, the Ba and the corresponding *Ln* translation modes shift to lower frequency by about 4 and 20–30 cm^{-1}, respectively. Jianmin *et al.* (*39*) studied the Fe-doped Y-123 and assigned the observed peaks whereas Song *et al.* (*40*) reported the IR reflectivity for Zn-doped Y-123. In the latter case, the dopant concentration was small and the compounds retained metallicity and superconductivity. Since all the $LnBa_2Cu_2CoO_{7+\delta}$ phases presently studied are semiconducting in nature, it is interesting to study the effect of chemical substitution at Y on the spectra of $YBa_2Cu_2CoO_{7+\delta}$. Further, the unobserved bands in the orthorhombic phase of $LnBa_2Cu_3O_{7+\delta}$ must be observed in these Co-doped orthorhombic semiconducting phases. For the $LnBa_2Cu_2CoO_{7+\delta}$ phases, due to the orthorhombic structure and partial occupation of Cu by Co, we expect to see more number of bands compared to $LnBa_2Cu_3O_6$. Indeed we observe several shoulders and fine structures in addition to the bands observed for $LnBa_2Cu_3O_6$. The results are discussed below. We could not obtain a well-resolved spectrum for the $LaBa_2Cu_2CoO_{7+\delta}$ phase due to its high conductivity compared to other phases.

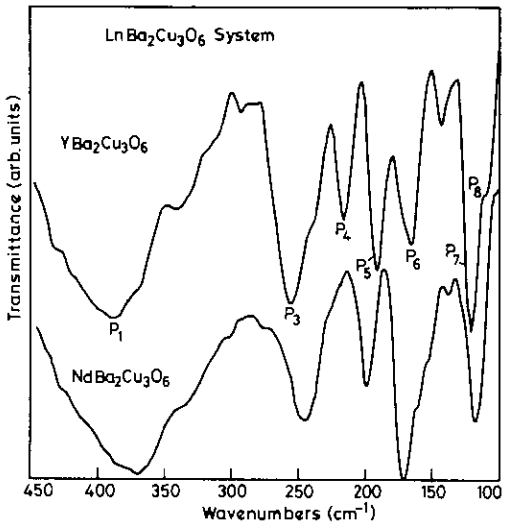

FIG. 2. Far-infrared diffuse reflectance spectra of $LnBa_2Cu_3O_6$ (Ln = Y, Nd) from 450–100 cm^{-1} at 300 K. When Y is replaced by Nd the modes at 218 and 193 cm^{-1} shift to 201 and 172 cm^{-1}, respectively.

The spectra of $YBa_2Cu_3O_6$, $NdBa_2Cu_3O_6$ and select samples of $LnBa_2Cu_2CoO_{7+\delta}$ in the region 450–100 cm^{-1} are shown in Fig. 2 and Fig. 3, respectively, and a summary of the assignments is listed in Table III. The oxygen deficient phases have been synthesized and characterized by XRD (see experimental). The oxygen content, estimated by iodometry, is found to be close to 6.0 (±0.03). The observed band positions of $YBa_2Cu_3O_6$ and $NdBa_2Cu_3O_6$ (Fig. 2) are in agreement with the results reported in the literature (*32, 34*). Several weak bands and shoulders are also noted in our spectra. In the spectra of $YBa_2Cu_3O_6$ and $NdBa_2Cu_3O_6$, the broad band seen in the region 420–350 cm^{-1} (peak P_1) and centered at 390 and 373 cm^{-1}, respectively, can be assigned to Cu(2)–O(2) in-plane bending mode. This doubly degenerate mode should split into B_{2u} and B_{3u} mode in the orthorhombic symmetry. In $LnBa_2Cu_2CoO_{7+\delta}$ (Fig. 3), in the region 420–350 cm^{-1} we see a broad band with reduced intensity and fine structure. Since the Cu(2)-site is partially occupied by Co, we expect a band due to the Co(2)–O(2) in-plane bending mode (E_u). The fine structure observed in the broad band could be due to the lifting of the degeneracy of the Cu(2)–O(2) and Co(2)–O(2) in-plane bending modes. The reduced intensity of the band can be understood as due to the high conductivity of the Co-doped phases compared to that of the undoped $LnBa_2Cu_3O_6$. A shoulder-like band seen clearly at 433 and 430 cm^{-1} for $YBa_2Cu_3O_6$ and $NdBa_2Cu_3O_6$, respectively, can be assigned to the Cu(1)–O(4) in-plane bending mode (*34*).

The Cu(2)–O(2) out-of-plane bending mode is symmetry-allowed only in the orthorhombic structure. Hence, this mode is IR-inactive in the tetragonal $LnBa_2Cu_3O_6$. For $YBa_2Cu_3O_7$ this mode is observed at 312 cm^{-1} (*34*). The broad band with fine structure observed between 330 and 280 cm^{-1} (peak P_2) in the orthorhombic Co-

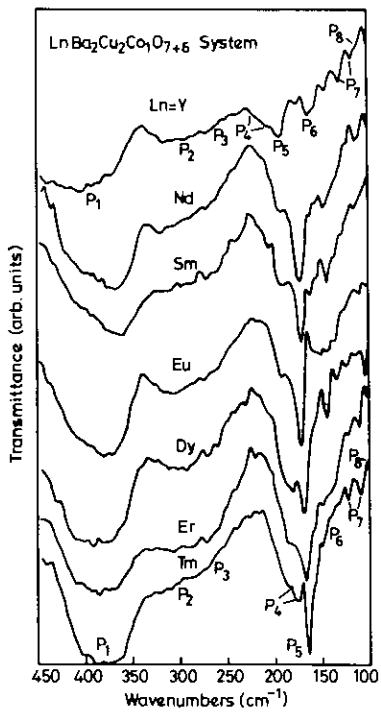

FIG. 3. Far-infrared diffuse reflectance spectra of $LnBa_2Cu_2CoO_{7+\delta}$ from 450–100 cm^{-1} at 300 K. Shifting of the Ln and Ba translational modes to lower frequency when Y is replaced by other heavier rare earths is evident. Appearance of the degeneracy-lifted modes (peaks P_4 and P_7) are also seen clearly (see text).

TABLE III

OBSERVED IR BANDS AND ASSIGNMENTS OF THE VIBRATIONAL MODES IN $LnBa_2Cu_3O_6$ AND $LnBa_2Cu_2CoO_y$ (Ln = Y, Rare earth)

Compound	Assignment[a] (cm^{-1})							
	P_1	P_2	P_3	P_4	P_5	P_6	P_7	P_8
$YBa_2Cu_3O_6$[b]	420–350 (cent. at 390)	Inactive	258	218	193	168	121	108
$NdBa_2Cu_3O_6$[b]	420–350 (cent. at 373)	Inactive	247	201	172	164(sh)	118	—
$LnBa_2Cu_2CoO_y$								
Ln = Y	420–350[c]	320–280[c]	275–250[c]	220, 207[d]	194	175–145[d]	130, 117	111
Nd	420–350	320–290	275–240	207, 193	172	165–145	124, 113	110
Sm	410–350	320–280	275–240	206, 193	172	165–136	129, 115	105
Eu	410–350	330–280	275–240	200, 192	173	165–136	125, 110	102
Dy	420–350	330–285	275–240	188, 182	171	165–134	124, 112	104
Ho	415–350	330–290	285–250	189, 179	170	165–135	122, 108	103
Er	420–350	330–285	275–240	186, 175	168	135–135	122, 111	101
Tm	410–350	330–290	280–240	188, 176	166	165–130	122, 109	102

[a] P_1: Cu(2)–O(2)/Co(2)–O(2) in-plane bend; P_2: Cu(2)–O(2)/Co(2)O(2) out-of-plane bend; P_3: Cu(2)–O(3)/Co(2)–O(3) out-of-plane bend; P_4: Ln translation in ab plane; P_5: Ln translation parallel to c; P_6: O(1)–Cu(1)/Co(1)–$(O(4))_2$–O(1) translation along c; P_7: Ba translation in the ab-plane; P_8: Ba translation parallel to c. The numbering of atoms in the 123 structure is discussed in the Introduction.

[b] Samples prepared by the vacuum method and characterized by XRD and iodometry (see text).

[c] Broad absorption with structure.

[d] Band splitting due to orthorhombicity similar to Y-$123O_7$ (see text).

doped phases may be due to the Cu(2)–O(2) and Co(2)–O(2) out-of-plane bending mode. The sharp intense band observed at 258 cm^{-1} (peak P_3) in $YBa_2Cu_3O_6$ is shifted to 247 cm^{-1} in $NdBa_2Cu_3O_6$. This band has been assigned to the Cu(2)–O(3) out-of-plane bending mode. In the Co-doped phases the corresponding band is not seen clearly; instead, a very broad band with fine structure is seen in the region 275–240 cm^{-1}. As mentioned earlier, the increased conductivity and partial occupation of Cu(2)-site by Co may be the reason for the broadness of the band and appearance of fine structure. We are not able to assign these fine structure bands unequivocally (Table III and Fig. 2).

The Y-translational mode in the ab-plane is doubly degenerate in the tetragonal $YBa_2Cu_3O_6$ and should split into B_{2u} and B_{3u} modes in the orthorhombic symmetry. For $YBa_2Cu_3O_6$ we observe this mode at 218 cm^{-1} (peak P_4). For $NdBa_2Cu_3O_6$, this mode shifts to lower frequency, as expected, and is observed at 201 cm^{-1}. Since the Co-doped phases are orthorhombic, we expect to see two bands corresponding to this mode of vibration. For $YBa_2Cu_2CoO_{7+\delta}$ we observe the Y-translation mode perpendicular to the c-axis at 220 and 207 cm^{-1}. As we substitute Y by other heavier rare earths we observe a shift in the frequency to the lower region (Table III). The sharp intense band seen at 193 cm^{-1} (peak P_5) in the spectra of $YBa_2Cu_3O_6$ can be assigned to Y translation along c-axis. As in the case of Y translation in the ab-plane, this mode also undergoes large shift in energy when rare earths are substituted for Y. For $NdBa_2Cu_3O_6$, this mode is observed at 172 cm^{-1}. Since it is not a degenerate mode, we do not expect any change in the energy of Ln translation along the c-axis in the corresponding Co-doped phases as well. For $LnBa_2Cu_2CoO_{7+\delta}$, Ln = Y and Nd we observe sharp intense

bands at 194 and 172 cm^{-1}, respectively, as expected (unshifted 193 and 172 cm^{-1} bands of $LnBa_2Cu_3O_6$, Ln = Y, Nd). This shift in frequency for different rare earths is due to change in force constants and unit cell dimensions (*34*). When Nd is substituted by other rare earths this mode either remains unaffected or shifts to lower frequency by about 6 cm^{-1} for Ln = Eu–Tm.

The vibrational mode corresponding to O(4)–Cu(1)–O(4) translation appears as sharp and intense band at 168 cm^{-1} (peak P_6) in $YBa_2Cu_3O_6$. For $NdBa_2Cu_3O_6$, however, we observe this mode as a shoulder at 164 cm^{-1}. In orthorhombic $YBa_2Cu_3O_7$, the mode corresponding to this is the O(1)–Cu(1)–$(O(4))_2$–O(1) translation along the c-axis, which appears at a lower frequency (155 cm^{-1}) (*34*). In $LnBa_2Cu_2CoO_{7+\delta}$, Co predominantly occupies the Cu(1) site. Hence, we expect O(1)–Co(1)–$(O(4))_2$–O(1) translation along the c-axis as an additional contribution. In $YBa_2Cu_2CoO_{7+\delta}$ we observe several small-intensity bands in the 175–145 cm^{-1} region and for $LnBa_2Cu_2CoO_{7+\delta}$ in the 165–130 cm^{-1} region. These are not unequivocally assignable to any of the above-mentioned modes.

In the spectrum of $YBa_2Cu_3O_6$ we observe a sharp band at 144 cm^{-1} (Fig. 2). Crawford *et al.* (*34*) observe only a shoulder in this region in their spectrum for $LnBa_2Cu_3O_6$ and attributed this shoulder and additional fine structure in this region (155–140 cm^{-1}) as possibly due to the vibrations involving residual oxygen at the chain sites in $LnBa_2Cu_3O_{6+\delta}$. In $NdBa_2Cu_3O_6$ we observe a clear but less intense band at 139 cm^{-1}.

The sharp intense band observed at 121 cm^{-1} (peak P_7) for $YBa_2Cu_3O_6$ is definitely due to the doubly degenerate Ba-translation mode in the *ab*-plane. In the orthorhombic symmetry this is expected to split as B_{2u} + B_{3u} modes. Like the Ln-translation modes, the Ba-translation modes also should shift to lower frequency when Y is substituted by heavy rare earths in $YBa_2Cu_3O_6$ and, indeed, we observe this mode at 118 cm^{-1} in $NdBa_2Cu_3O_6$. In $YBa_2Cu_2CoO_{7+\delta}$ the less intense bands at 130 and 117 cm^{-1} can be assigned to the degeneracy-lifted mode of the Ba-translation in the *ab*-plane. For the other $LnBa_2Cu_2CoO_{7+\delta}$ phases, these modes are shifting to lower frequencies as expected, more or less in a systematic fashion. The shoulder-like band observed at 108 cm^{-1} (peak P_8) for $YBa_2Cu_3O_6$ (but not seen in $NdBa_2Cu_3O_6$) can be assigned to Ba-translation along the c-axis (*34*). In the Co-doped phases also this band appears either as a shoulder or a well-defined band and undergoes systematic changes to lower energy values when Y is replaced by other rare earths (Table III and Fig. 3).

To summarize, far-IR studies show that our results for the $LnBa_2Cu_3O_6$ phases are in agreement with those reported in the literature. We observe strong, intense bands for the semiconducting, tetragonal $LnBa_2Cu_3O_6$ phases. The Co-doped phases are orthorhombic and are semiconducting. Still, their conductivity is much higher than that of the $LnBa_2Cu_3O_6$ phases and hence due to the interference of the conduction electrons we observe broad bands with reduced intensity. The bands due to the splitting of the doubly degenerate Ln-translation in the *ab*-plane and Ba-translation in the *ab*-plane are clearly seen in our $LnBa_2Cu_2CoO_{7+\delta}$ spectra. This is a clear indication of the orthorhombic nature of the Co-doped phases. As Y is substituted by other rare earths the corresponding Ln- and Ba- translational modes also shift to lower frequencies as expected. The spectrum of tetragonal $TmBa_2Cu_2CoO_{7+\delta}$ appears to be similar to that of other orthorhombic $LnBa_2Cu_2CoO_{7+\delta}$. This is probably due to the existence of orthorhombic microdomains, as discussed earlier.

d. Electrical and Magnetic Properties of $LnBa_2Cu_2MO_{7+\delta}$ (M = Ga,Co)

Electrical resistivity studies were done on single phase, oxygen annealed pellets. For $LnBa_2Cu_2GaO_{7+\delta}$ phases resistivity (ρ) vs temperature (T) studies were done by the two-probe method in the range 303–480 K.

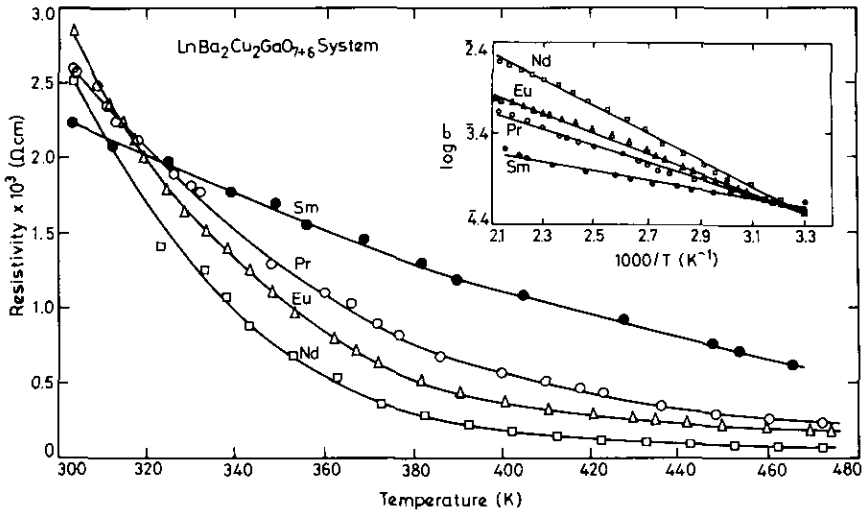

Fig. 4. Resistivity vs temperature plots for LnBa$_2$Cu$_2$GaO$_{7+\delta}$ (Ln = Pr, Nd, Sm, Eu) showing semiconducting behavior (two probe measurement). Inset shows log σ vs 1000/T plots for the phases for estimation of E_a.

Four-probe measurements could not be carried out due to significant fluctuations in voltage drop (both with In-soldered or with Ag-paint contacts) even for small values of impressed current (0.1 mA). This behavior appears to be an inherent property of the material. Similar observations were also made during our studies on the NdBa$_2$Cu$_{3-x}$Ga$_x$O$_7$ phases wherein the difficulty in estimating ρ by the four probe measurements increases with increasing Ga content (x) (*21*). The resistivity at each temperature was calculated using the relation $\rho = R \times A/l$, where R is the measured resistance (ohms), A and l are the area of cross section and thickness of the pellets, respectively. ρ vs T plots of LnBa$_2$Cu$_2$GaO$_{7+\delta}$ phases are shown in Fig. 4. All the phases are semiconducting in the temperature range measured. The room temperature resistivities of the Ga-containing phases are of the order of kΩ cm for all the Ln-phases (Table I). The ρ vs T plots are fitted to an Arrhenius-type equation, $\sigma = \sigma_0 \exp(E_a/kT)$ in the temperature range 303–480 K, where $\sigma = 1/\rho$. The energies of activation (E_a) for conduction in this temperature range are calculated from the slope of the log σ vs $1/T$ plots (Fig. 4, inset). The E_a values are in the range 0.10–0.28 eV (Table I). Measurements below 300 K could not be carried out due to the high resistance of the samples.

For the LnBa$_2$Cu$_2$CoO$_{7+\delta}$ phases, ρ–T studies were done on oxygen-annealed pellets by four-probe van der Pauw method. All the phases exhibit semiconducting behavior in the range 300–150 K. Below 150 K, measurements could not be done due to fluctuations in voltage drop while passing current. The room temperature four-probe resistivity values ($\rho_{300\ K}$) are in the range 0.02–40 Ω cm and are much lower than that of the corresponding Ga-doped phases (two-probe measurements). There are no systematics in the $\rho_{300\ K}$ values as a function of rare earth ion, possibly due to the polycrystalline nature of the samples (Table II). Figure 5 shows log σ vs $1/T$ plots for select phases in the LnBa$_2$Cu$_2$CoO$_{7+\delta}$ system. The activation energy values for conduction calculated using Arrhenius equation for the range 300–150 K are given in Table II. LaBa$_2$Cu$_2$CoO$_{7+\delta}$ shows minimum activation energy (0.03 eV). For all the other LnBa$_2$Cu$_2$CoO$_{7+\delta}$ phases, the E_a values are in the range 0.06–0.18 eV.

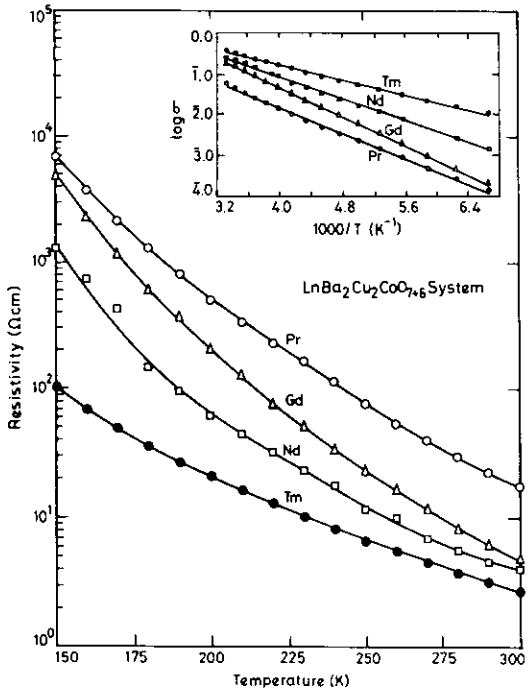

FIG. 5. Resistivity vs temperature plots for $Ln Ba_2Cu_2CoO_{7+\delta}$ (Ln = Pr, Nd, Gd, Tm) showing semiconducting behavior. Inset shows log σ vs $1000/T$ plots for the phases.

The metallic conduction and superconductivity in $YBa_2Cu_3O_{7-\delta}$ is explained by considering CuO chains as charge reservoirs and charge transfer to the CuO_2-planes is effected via the bridging oxygen, O(4). Thus, mobile charge carriers (holes) are created in the CuO_2 planes and the observed p-type metallic conduction and superconductivity are due to these carriers in the CuO_2 planes. Decrease in the oxygen content decreases the hole concentration (due to reduction of Cu^{3+}) and the metallicity decreases. The T_c also decreases and the compound shows semiconducting behavior and no superconductivity is encountered for $\delta > 0.6$–0.65 (*1–4, 41*). It is known that substitution at the Cu-site (Cu(1) as well as Cu(2)) leads to loss of metallicity as well as superconductivity (*10–12*). In the present study, the Cu^{3+} (formal valency) of $Ln Ba_2Cu_3O_7$ is completely replaced by Ga^{3+} which has a filled $3d^{10}$ configuration (fixed valency of 3+) to form $Ln Ba_2Cu_2GaO_7$. Since the oxygen content remains at 7.0 (and does not increase beyond 7.0), the formal oxidation state of remaining Cu is only +2. Thus, there is no scope for the creation of holes and hence the observed semiconducting behavior. In $Ln Ba_2Cu_2CoO_{7+\delta}$ also the Cu^{3+} is completely replaced by Co^{3+}. However, unlike in the case of Ga-substituted phases, the oxygen stoichiometry increases above 7.0 (~7.28). The excess oxygen should oxidize some Cu^{2+} to Cu^{3+} thereby creating charge carriers (holes). However, the compounds do not exhibit metallic behavior and superconductivity.

The total hole concentration consists of two components, the localized and the mobile holes. The concentration of the mobile holes determines the conductivity of the compound. Clayhold *et al.* (*42*) have shown from Hall-effect measurements that in $YBa_2Cu_{3-x}Co_xO_{7+\delta}$ the carrier density (mobile hole density) decreases exponentially with increasing x. Although superconductivity is largely determined by conduction in CuO_2-planes, the substitution of Co in the CuO chains will lead to a redistribution of charge carriers (holes) in the chain region and possibly to an inhibition of charge transfer from the chains to the planes. Neutron diffraction studies on the $YBa_2Cu_{3-x}Co_xO_{7+\delta}$ system (*43*) reveal a dramatic change in the Cu(1)–O(4) bond length. The apical oxygen [O(4)] is progressively drawn away from CuO_2 planes with increasing x. This leads to an exponential decrease in the overlap integral between Cu(2) $3d_{z^2}$ and O(4) $2p_z$ states with increasing x and therefore an exponential decrease in the number of mobile carriers leading to not only suppression of T_c but also onset of semiconducting behavior. Thus, the semiconductivity in Ga- and Co-substituted phases is due to the decrease in mobile charge carriers.

The temperature dependence of the magnetic susceptibility (χ vs T) was studied for the $Ln Ba_2Cu_2GaO_{7+\delta}$ phases (Ln = Pr, Nd, Sm, Gd) using a SQUID magnetometer in the range 300–5 K in a field of 100 G. The

reciprocal susceptibility vs temperature ($1/\chi$ vs T) plots in the range 300–100 K could be fitted to a Curie–Weiss law except when Ln = Sm. Below 100 K the $1/\chi$ vs T plots for Ln = Pr and Nd show deviation from linearity caused by the crystalline electric field (CEF) splitting effects. The nonlinearity in the case of Ln = Sm in the temperature range 300–5 K is also due to crystalline electric field effects (*44*). The values of Weiss constants (θ) are 28, 33.5, and 2.4 K for Ln = Pr-, Nd-, and Gd-phases, respectively. The values of the effective magnetic moment (μ_B) calculated from the values of C (Curie constant) are in good agreement with the free-ion moments of Pr^{+3}, Nd^{+3} and Gd^{+3} (*45, 46*) (Table I). Sunshine *et al.* (*14*), from their magnetic susceptibility measurements, observed antiferromagnetic behavior in the semiconducting samples in the system $YSr_2Cu_{3-x}Al_xO_7$. Indeed, $YSr_2Cu_2AlO_7$ shows a Néel temperature of 11 K. In the present study, however, such ordering of Cu moments is not observed for any of the phases. More detailed studies at higher fields are required and are currently under way.

Summary

The effect of varying the rare earth ion (Ln) in the $LnBa_2Cu_2MO_{7+\delta}$ (M = Ga and Co) system on the phase formation and structural features is studied. In the $LnBa_2Cu_2GaO_{7+\delta}$ system, single-phase formation is observed only when Ln = La–Eu. All the single phase compounds possess tegragonal 123 structure and the oxygen content is found to be ~7.0. In the $LnBa_2Cu_2CoO_{7+\delta}$ system single-phase formation is observed for Ln = La–Tm and Y, and the oxygen content is 7.25 ± 0.03 for all the phases. The phases with Ln = La–Er are orthorhombic and the Y-analogue is almost tetragonal. When Ln = Tm the phase is tetragonal. Thus, our studies show that the phase formation and structural features of the Co- and Ga-substituted Ln-123 system depend very much on the size of the lanthanide ion. Far-infrared diffuse reflectance studies show that when Y is replaced by other heavier lanthanides, the corresponding Ln-translational modes and Ba-translational modes shift to lower frequency systematically, as expected. The degenerate modes in the $LnBa_2Cu_3O_6$ spectra appear as split modes in the $LnBa_2Cu_2CoO_{7+\delta}$ spectra, proving that the phases are indeed orthorhombic in structure. All the phases are found to be semiconducting with activation energies in the range 0.03–0.28 eV. Magnetic susceptibility measurements done on select samples of $LnBa_2Cu_2GaO_{7+\delta}$ phases show that the effective magnetic moments obtained for the trivalent lanthanide ions are in agreement with the free-ion values reported in the literature and are unaffected by the presence of Ga at the Cu-site.

Acknowledgments

Thanks are due to Professor G. V. Subba Rao for valuable discussions and critical reading of the manuscript. Thanks are also due to the Natl. Sci. & Tech. Board (NSTB) on Superconductivity of DST, Govt. of India, New Delhi, for a research grant.

References

1. C. N. R. Rao (Ed.), "Chemical and Structural Aspects of High Temp. Supercond.," World Sci., Singapore (1988); C. N. R. Rao (Ed.), "Chemistry of Oxide Supercond.," Blackwell, Oxford (1988); A. K. Gupta, S. K. Joshi, and C. N. R. Rao (Eds.), "Proc. of Srinagar Workshop on High Temp. Supercond., Srinagar, India, 1988," World Sci., Singapore (1988).
2. K. Kitazawa and T. Ishiguro (Eds.), "Adv. in Supercond., Proc. of 1st Intl. Symp. on Supercond. Nagoya," Springer-Verlag, Tokyo (1988).
3. C. N. R. Rao, *J. Solid State Chem.* **74,** 147 (1988); T. V. Ramakrishnan and C. N. R. Rao, *J. Phys. Chem.* **93,** 4414 (1989); C. N. R. Rao and B. Raveau, *Acc. Chem. Res.* **22,** 106 (1989); C. N. R. Rao (Ed.), "Chemistry of High Temp. Supercond.," World Sci., Singapore (1991).
4. A. V. Narlikar (Ed.), "Studies on High Temp. Superconductors," Vols. 1–7, Nova, New York (1989–1991).
5. C. N. R. Rao, R. Nagarajan, A. K. Ganguli, G. N. Subbanna, and S. V. Bhat, *Phys. Rev. B* **42,** 6765 (1990).
6. C. J. Hou, A. Manthiram, L. Rabenberg, and J. B. Goodenough, *J. Mater. Res.* **5,** 9 (1990).

7. Y. Hariharan, C. S. Sunder, J. Janaki, A. K. Sood, M. P. Janawadkar, A. Bharathi, V. Sankara Sasatry, R. Baskaran, and T. S. Radhakrishnan, *in* "Studies in High Temp. Superconductors," Vol. 3, pp. 107–141, Nova, New York (1990).
8. P. Somasundaram, K. S. Nanjundaswamy, A. M. Umarii, and C. N. R. Rao, *Mater. Res. Bull.* **23,** 1139 (1988).
9. T. J. Kistenmacher, *Phys. Rev. B* **38,** 8862 (1988).
10. J. M. Tarascon, P. Barboux, P. F. Miceli, L. H. Greene, G. W. Hull, M. Eibschutz, and S. A. Sunshine, *Phys. Rev. B* **37,** 7458 (1988).
11. B. D. Dunlap, J. D. Jorgensen, W. K. Kwok, C. W. Kimball, J. L. Matykiewicz, H. Lee, C. U. Segre, and A. E. Dwight, *Physica C* **153–155,** 1100 (1988); B. D. Dunlap, J. D. Jorgensen, C. U. Segre, A. E. Dwight, J. L. Matykiewicz, H. Lee, W. Peng, and C. W. Kimball, *Physica C* **158,** 397 (1989).
12. Y. Maeno and T. Fujita, *Physica C* **153–155,** 1105 (1988).
13. G. Xiao, M. Z. Cieplak, D. Musser, A. Gavrin, F. H. Streitz, C. L. Chien, J. J. Rhyne, and J. A. Gotaas, *Nature* **332,** 238 (1988); G. Xiao, M. Z. Cieplak, A. Gavrin, F. H. Streitz, A. Bakhshai, and C. L. Chien, *Phys. Rev. Lett.* **60,** 1446 (1988).
14. S. A. Sunshine, L. F . Schneemeyer, T. Siegrist, D. C. Douglass, J. V. Waszczak, R. J. Cava, E. M. Gyorgy, and D. W. Murphy, *Chem. Mater.* **1,** 331 (1989).
15. G. Roth, P. Adelmann, G. Heger, R. Knitter, Th. Wolf, *J. Physique* **1,** 721 (1991).
16. J. T. Vaughey, J. P. Thiel, E. F. Hasty, D. A. Groenke, C. L. Stern, K. R. Poeppelmeier, B. Dabrowski, D. G. Hinks, and A. W. Mitchell, *Chem. Mater.* **3,** 935 (1991).
17. N. Murayama, E. Sudo, K. Kani, A. Tsuzuki, S. Kawakami, M. Awano, and Y. Torri, *Jpn. J. Appl. Phys.* (*2*) **27,** L1623 (1988).
18. C. Greaves and P. R. Slater, *Physica C* **161,** 245 (1989).
19. M. J. Rey, Ph. Dehaudt, J. Joubert, and A. W. Hewat, *Physica C* **167,** 162 (1990).
20. U. Yaron, D. Kowal, I. Felner, and M. Einav, *Physica* **168,** 546 (1990).
21. T. A. Mary and U. V. Varadaraju, *Mater. Res. Bull.* **27,** 447 (1992).
22. A. I. Nazzal, V. Y. Lee, E. M. Engler, R. D. Jacowitz, Y. Tokura, and J. B. Torrance, *Physica C* **153–155,** 1367 (1988); Y. Maeno, H. Teraoka, K. Matsukuma, K. Yoshida, K. Sugiyama, F. Nakamura, and T. Fujita, *Physica C* **185–189,** 587 (1991).
23. F. Bridges, J. B. Boyce, T. Claeson, T. H. Geballe and J. M. Tarascon, *Phys. Rev. B* **42,** 2137 (1990).
24. Z. Hiroi, M. Takano, Y. Takeda, R. Kanno, and Y. Bando, *Jpn. J. Appl. Phys.* **27,** L580 (1988); J. L. Hodeau, P. Bordett, J. J. Capponi, C. Chaillout, J. Chenavas, M. Hewat, E. A. Hewata, H. Reneveir, A. M. Spieser, P. Strobel, J. L. Tholence, and M. Marezio, *in* "Progress in High Temp. Superconductivity," Vol. 12, p. 159, World Scientific, Singapore (1988).
25. G. Roth, G. Heger, B. Renker, J. Pannetier, V. Caignaert, M. Hervieu, and B. Raveau, *Z. Phys. B.* **71,** 43 (1988).
26. Y. Xu, M. Suenaga, J. Tafto, R. L. Sabatini, A. R. Moodenbaugh, and P. Zolliker, *Phys. Rev. B* **39,** 6667 (1989).
27. P. R. Slater, A. J. Wright, and C. Greaves, *Physica C* **183,** 111 (1991).
28. J. M. Tarascon, R. Ramesh, P. Barboux, M. S. Hegde, G. W. Hull, L. H. Greene, M. Giroud, Y. LePage, W. R. Mckinnon, J. V. Waszczak, and L. F. Schneemeyer, *Solid State Commun.* **71,** 663 (1989).
29. V. Caignaert, N. Nguyen, and B. Raveau, *Mater. Res. Bull.* **25,** 199 (1990); B. Lakshmi Brinda, U. V. Varadaraju and G. V. Subba Rao, *Bull. Mater. Sci.* (*India*) **14,** 315 (1991).
30. T. A. Mary, N. R. S. Kumar, and U. V. Varadaraju, submitted for publication.
31. M. S. Hegde, S. Ramesh, and T. S. Panchapagesan, *J. Solid State Chem.* **102,** 306 (1993).
32. R. Feile, *Physica C* **159,** 1 (1989) and references therein.
33. F. E. Bates, *Phys. Rev. B* **39,** 322 (1989).
34. M. K. Crawford, W. E. Farneth, E. M. McCarron III, and R. K. Bordia, *Phys. Rev. B* **38,** 11382 (1988).
35. G. Burns, F. H. Dacol, P. P. Freitas, W. Konig, and T. S. Plaskett, *Phys. Rev. B* **37,** 5171 (1988).
36. C. Thomsen, M. Cardona, W. Kress, R. Liu, L. Genzel, M. Bauer, E. Schonherr, and U. Schroder, *Solid State Commun.* **65,** 1139 (1988).
37. H. Kuzmany, E. Faulques, M. Matus, and S. Pekker, *in* "Studies on High Temp. Superconductors," Vol. 3, pp. 299–326, Nova, New York (1990).
38. J. R. Fernandes, V. Varma, P. Ganguly, and C. N. R. Rao, *Mod. Phys. Lett. B* **2,** 517 (1988).
39. C. Jianmin, X. Leimin, Z. Yonggang, C. Peixin, and G. Huifang, *Physica C* **159,** 317 (1989).
40. Q. Song, B. P. Clayman, and S. Gygax, *Physica C* **165,** 328 (1990).
41. Z. Z. Wang, J. Clayhold, N. P. Ong, J. M. Tarascon, L. H. Greene, W. R. Mckinnon, and G. W. Hull, *Phys. Rev. B* **36,** 7222 (1987).
42. J. Clayhold, S. Hagen, Z. Z. Wang, N.P. Ong, J. M. Tarascon, and P. Barboux, *Phys. Rev. B* **39,** 777 (1989).

43. P. F. MICELI, J. M. TARASCON, L. H. GREENE, P. BARBOUX, F. J. ROTELLA, AND J. D. JORGENSEN, *Phys. Rev. B* **37,** 5932 (1988).

44. H. ZHOU, C. L. SEAMAN, Y. DALICHAOUCH, B. W. LEE, K. N. YANG, R. R. HAKE, M. B. MAPLE, R. P. GUERTIN, AND M. V. KURIC, *Physica C* **152,** 321 (1988).

45. G. XIAO, F. H. STREITZ, A. GAVRIN, AND C. L. CHIEN, *Solid State Commun.* **63,** 817 (1987).

46. M. A. ALARIO-FRANCO, E. MORAN-MIGUELEZ, R. SAEZ-PUCHE, F. GARCIA-ALVARADO, U. AMADOR, M. BARAHONA, F. FERNANDEZ, M. T. PEREZ-FRIAS, AND J. L. VINCENT, *Mater. Res. Bull.* **23,** 313 (1988).